2Pa5-15

Proceedings of Symposium on Ultrasonic Electronics, Vol. 32 (2011) pp. 163-164
8-10 November, 2011

Ultrasound Image Interpretation for Fibrotic Liver Based on Simulation Model of Tissue Structure Change

組織構造変化モデルに基づく線維化肝臓の超音波画像評価

Wataru Yasuhara[1†], Tadashi Yamaguchi[2], and Hiroyuki Hachiya[1]
([1]Tokyo Inst. of Tech.; [2] Chiba Univ.)
安原　航[1†]，山口　匡[2]，蜂屋　弘之[1] ([1]東工大; [2]千葉大)

1. Introduction

We have examined a quantitative estimation technique for liver deseases using clinical ultrasonic echo data[1)-5)] and measured tissue acoustic structure[6)-7)]. We also proposed a scatterer distriubution model of fibrotic livers to examine the relation between B-mode image and tissue scatterer distribution[8)-10)]. In this paper, we present quantitative characteristics of echo image of fibrotic liver using pathological tissue image and simulated scatterer model. The validity of simulated scatterer model is discussed.

2. Scatterer Distribution of Fibrotic Liver

Figure 1(a) and **(b)** show pathological tissue images (30×30 mm). Since the pathological tissues were stained by Masson's trichrome stain method, as shown in **Fig. 1**, the collagen fibers were stained blue and the nuclei were stained black and the background was stained red. **Fig. 1(a)** shows B-virus related cirrhotic tissue image, and **Fig. 1(b)** shows non-B non-C cirrhotic tissue image. **Figure 2** shows distributed scatterers using pathological tissue image shown in **Fig. 1**. A fibrous tissue was extracted from pathological tissue image using color information. The scatterer density of extracted fibrosis tissue is seven times larger than that of other tissue.

We simulated scatterer distribution using proposed simulation model of fibrotic liver as shown in **Figure 3(a)** and **(b)**. The fibrous tissue ratio of **Fig. 2(a)** is 41.5%. **Fig. 3(a)** shows simulated scatterer distribution modeled for B-virus related cirrhosis (**Fig. 2(a)**). The fibrous ratio of **Fig. 3(a)** is 41.6%. **Fig. 2(b)** shows a scatterer distribution made from non-B non-C cirrhosis tissue image (**Fig. 1(b)**). The fibrous ratio of **Fig. 2(b)** is 60.0%. **Fig. 3(b)** shows simulated scatterer distribution modeled for non-B non-C cirrhosis (**Fig. 2(b)**). The fibrous ratio of **Fig. 3(b)** is 59.5%.

Then we calculated the B-mode images using the structures of scatterers in **Figs.2** and **3**.

3. Quantitative Characteristics of B-mode Image

Figures 4 and **5** show area distributions of

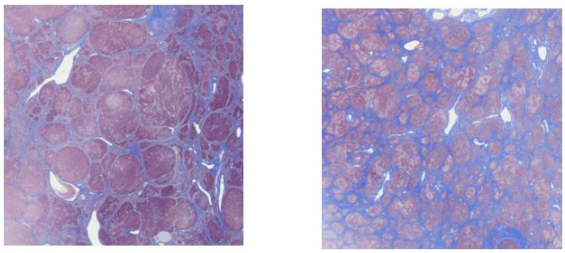

(a) B-virus related Cirrhosis　(b) non-B non-C Cirrhosis

Fig. 1　Pathological tissue image

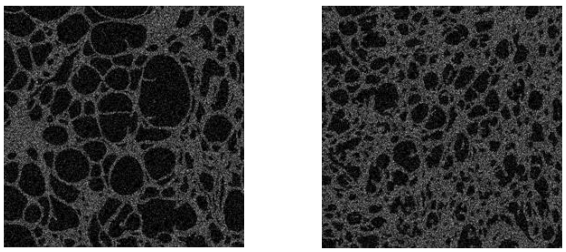

(a) B-virus related Cirrhosis　(b) non-B non-C Cirrhosis

Fig. 2　Scatterer distribution using Pathological image

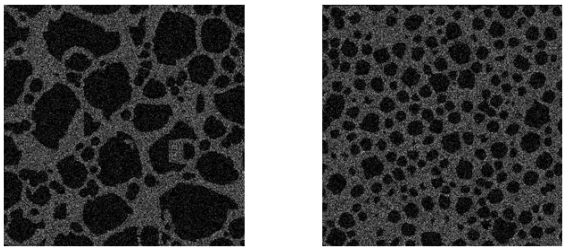

(a) B-virus related Cirrhosis　(b) non-B non-C Cirrhosis

Fig. 3 Simulated scatterer distribution

nodules on simulated scatterer. In **Figs. 4** and **5**, a nodule is defined by an area surrounded by fibrous tissue. **Figures 4(a)** and **(b)** show nodule area distributions of **Figs. 2(a)** and **3(a)**. **Figures 5(a)** and **(b)** show nodule area distributions of **Figs. 2(b)** and **3(b).** Area distributions of simulated results agree well with nodule area distributions in pathological images. From these figures, it is clear the parameters for scatterer distribution model can be controlled to simulate tissues of B-virus related cirrhosis and non-B non-C cirrhosis.

Figure 6 shows B-mode images calculated from scatterer structures in **Figs.2** and **3**. The center frequency is 5.0 MHz. The aperture and focal

†yasuhara@us.titech.ac.jp

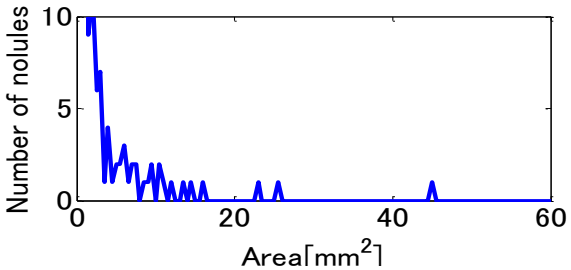

(a) Pathological type B cirrhosis

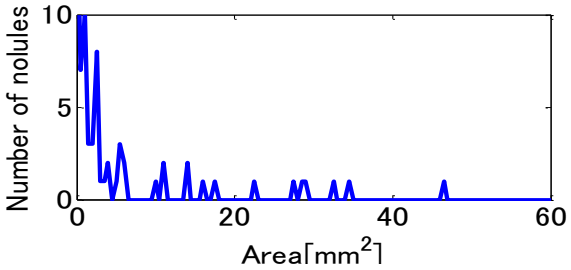

(b) Simulated type B cirrhosis

Fig. 4 Nodule area distribution(type B cirrhosis)

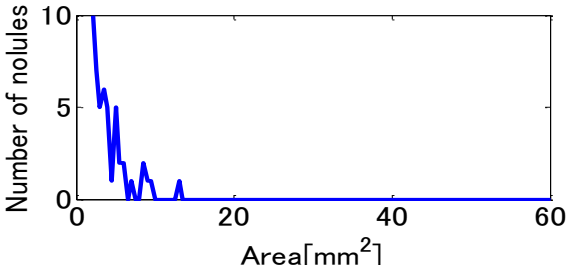

(a) Pathological non-B non-C

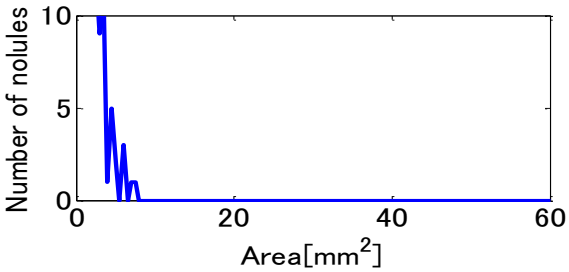

(b) Simulated non-B non-C

Fig. 5 Nodule area distribution(non-B non-C)

length of a transducer are 10 mm and 31.3 mm. **Figure 7** shows mean and variance of skewness calculated from the probability density function of simulated echo data (**Fig. 6**). Sixteen simulated echo images are calculated on the different random distributions using each condition of 1) pathological image (B-virus), 2) simulation (B-virus), 3) pathological image (non-B non-C) and 4) simulation (non-B non-C)). The skewnesses calculated from simulated echo data agree well with the skewnesses of echo signal of pathological data.

4. Conclusion

We have presented quantitative characteristics of echo image of fibrotic liver using pathological

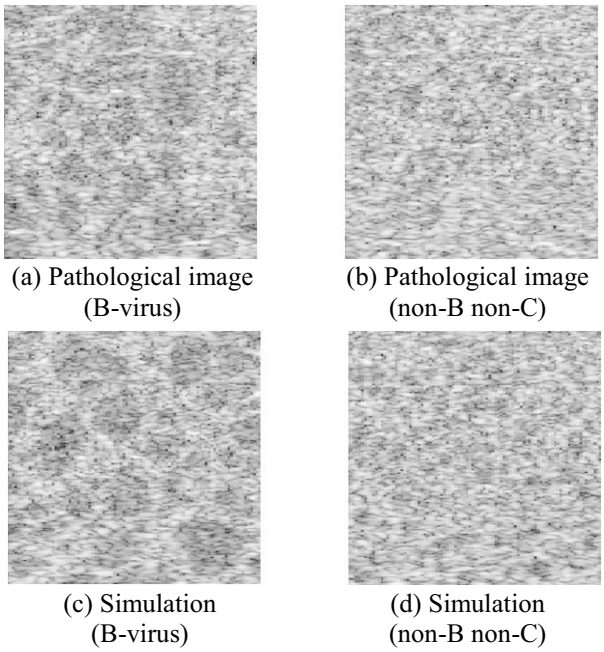
(a) Pathological image (B-virus)

(b) Pathological image (non-B non-C)

(c) Simulation (B-virus)

(d) Simulation (non-B non-C)

Fig. 6 B-mode image

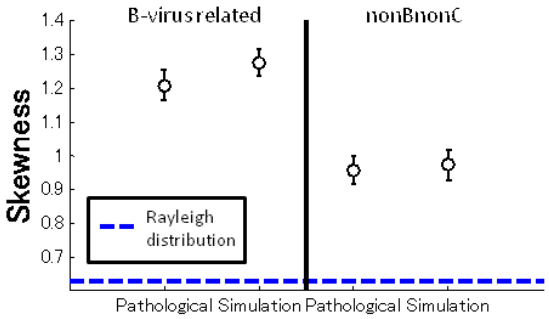

Fig. 7 Skewness of B-mode image

tissue image and simulated scatterer model. The proposed scatterer distribution model of fibrotic livers can simulate pathological tissue. This model is valid to interpret ultrasonic image of fibrotic liver.

Acknowledgment

This work was supported by Grant-in-Aid for Scientific Research on Innovative Areas.

References

1. T. Yamaguchi, H. Hachiya, Jpn. J. Appl. Phys., 37, 3093-3096, 1998.
2. T. Yamaguchi, et. al., Jpn. J. Appl. Phys., 40, 3900-3904, 2001.
3. T. Yamaguchi, H. Hachiya, J. Med. Ultrasonics 37, 155–166 , 2010.
4. Y. Igarashi, et al., Jpn. J. Appl. Phys., 49, 07HF06, 2010.
5. Y. Igarashi, et al, Jpn. J. Appl. Phys., 50, 07HF17, 2011.
6. H. Hachiya, et al.: J. Acoust. Soc. Am., **92**(3), 1564, (1992).
7. H. Hachiya, et al.: Jpn. J Appl. Phys., **33**, 3130 , 1994.
8. T. Yamaguchi, et al.: Jpn. J. Appl. Phys., **38**, 3388, 1999.
9. T. Hara, et al.: Jpn. J. Appl. Phys., **39**, 3262, 2000.
10. T. Yamaguchi, et al.: Jpn. J. Appl. Phys., **42**, 3292, 2003.